On the compressibility effect in test particle acceleration by magnetohydrodynamic turbulence

C.A. González,[1, a)] P. Dmitruk,[1] P.D. Mininni,[1] and W.H. Matthaeus[2]
[1)] *Departamento de Física, Facultad de Ciencias Exactas y Naturales, Universidad de Buenos Aires and IFIBA, CONICET, Ciudad universitaria, 1428 Buenos Aires, Argentina*
[2)] *Bartol Research Institute and Department of Physics and Astronomy, University of Delaware, Newark, Delaware, USA*

The effect of compressibility in charged particle energization by magnetohydrodynamic (MHD) fields is studied in the context of test particle simulations. This problem is relevant to the solar wind and the solar corona due to the compressible nature of the flow in those astrophysical scenarios. We consider turbulent electromagnetic fields obtained from direct numerical simulations of the MHD equations with a strong background magnetic field. In order to explore the compressibilty effect over the particle dynamics we performed different numerical experiments: an incompressible case, and two weak compressible cases with Mach number $M = 0.1$ and $M = 0.25$. We analyze the behavior of protons and electrons in those turbulent fields, which are well known to form aligned current sheets in the direction of the guide magnetic field. We show that compressibility enhances the efficiency of proton acceleration, and that the energization is caused by perpendicular electric fields generated between currents sheets. On the other hand, electrons remain magnetized and they show an almost adiabatic motion, with no effect of compressibility observed.

I. INTRODUCTION:

Turbulence is an ubiquitous phenomenon in many astrophysical environments in which a wide variety of temporal and spatial scales are involved. This is the case of the solar wind or the intellestar medium where the energy is transferred from large to small kinetic scales where the energy is dissipated. Turbulence is the result of the nonlinear interaction of fluctuations of the velocity and magnetic fields, leading to a spatial intermittency that is associated with coherent structures, and where the dissipation is concentrated in strong gradient regions that impact on the heating, transport and particle acceleration in plasmas[15].

The efficiency of magnetohydrodynamics (MHD) turbulence to accelerate charged particles and its importance in space physics has been reported by many different authors[10,12,14], but the great variety of scales involved in turbulence and the particle dynamics makes this a challenging problem. On long timescales (large eddy turnover times) dynamics is governed by stochastic acceleration, and momentum diffusion is the main acceleration mechanism which has been mainly applied for cosmic-ray energization studies and frequently addressed by quasi-linear theory (QLT)[4,11,17]. In diffusion studies MHD turbulence is commonly represented as a random collection of waves, and that representation lacks of coherent structures that have an important role at particle scales[2]

Dmitruk et al 2004[8], using test particle simulations in static electromagnetic fields obtained from direct numerical simulation (DNS) of the MHD equations, showed that particle energization at dissipation scales is due to current sheets, and thet the acceleration mechanism depends on the particle gyroradii. By static electromagnetic fields, here we mean that the fields are dynamically computed in a turbulent and self-consistent MHD simulation, and then a snapshot is extracted and the fields are frozen to compute particle trajectories and acceleration.

Using a more sophisticated model, but still using static turbulent electromagnetic fields, Dalena et al 2012[7] showed essentially the same results. Electrons initially moving with Alfvén velocity experience parallel (to the guide magnetic field) acceleration by parallel electric fields inside current sheet chanels. On the other hand, protons are accelerated in a two stage process: Initially they are parallelly accelerated and gain substantial energy in a short time. Then, when the proton gyroradius becomes comparable to the current sheet thickness, and protons are accelerated perpendicular to the guide field.

Effects of compressible MHD on particle energization has been reported in diffusion studies[3,5], where supersonic turbulence was considered. There are also reports of test particle pitch angle scattering in compressible MHD turbulence. Lynn et al 2013[13] considering second order Fermi acceleration by weak compressible MHD running simultaneously the test particles and MHD fields, and imposing a scattering rate. It was found that compressibility is important to produce non-thermal particles.

Additionally, there are other studies where test particles and fields are simultaneously advanced in time. Weidl et al 2015[20] and Teaca et al. 2014[19] use an incompressible MHD model, analyzing the effect of the correlation between magnetic and velocity fields on pitch-angle scattering and particle acceleration. They found that imbalanced turbulence (nonzero cross-helicity in the sys-

[a)] Electronic mail: caangonzalez@df.uba.ar

tem) enhances the particle acceleration and also the pitch angle scattering.

In the present work we are interested in the compressibility effect on particle acceleration by coherent structures in static electromagnetic fields from a direct numerical simulation of the MHD equations, and in the identification of the fields which accelerate the particles. We analyze the particle behavior for three different situations: an incompressible case, and two weakly compressible cases with differing values of the sonic Mach number.

The organization of this paper is the following: In section 2 we describe the model employed in our investigation, the equations and properties of turbulent MHD fields, and the test particle model including the parameters that correlate particles and fields. In section 3 we show the properties of proton and electron dynamics. Finally in section 4 we discuss our findings and present our conclusions.

II. MODELS:

The macroscopic description of a plasma adoped here is the system of the three-dimensional compressible MHD equations: the continuity (density) equation, the equation of motion, the magnetic field induction equation, and the equation of state. These are Eqs. (1-4) respectively, which involve fluctuations of the velocity field $\mathbf{u}$, magnetic field $\mathbf{b}$, and density ρ. We assume a large-scale background magnetic field B_0 in the z-direction, so that the total magnetic field is $\mathbf{B} = \mathbf{B_0} + \mathbf{b}$

$$\frac{\partial \rho}{\partial t} + \nabla \cdot (\mathbf{u}\rho) = 0, \tag{1}$$

$$\frac{\partial \mathbf{u}}{\partial t} + \mathbf{u}\cdot\nabla\mathbf{u} = -\frac{\nabla p}{\rho} + \frac{\mathbf{j}\times\mathbf{B}}{4\pi\rho} + \nu\left(\nabla^2\mathbf{u} + \frac{\nabla\nabla\cdot\mathbf{u}}{3}\right), \tag{2}$$

$$\frac{\partial \mathbf{B}}{\partial t} = \nabla\times(\mathbf{u}\times\mathbf{B}) + \eta\nabla^2\mathbf{B}, \tag{3}$$

$$\frac{p}{\rho^\gamma} = \text{constant}. \tag{4}$$

Here p is the pressure, ν the viscosity, η the magnetic diffusivity, and $\mathbf{J} = \nabla\times\mathbf{B}$ is the current density. We assume a polytropic equation of state $p/p_0 = (\rho/\rho_0)^\gamma$, with $\gamma = 5/3$, and p_0, ρ_0 the equilibrium (reference) pressure and density. We consider two weak compressible cases with Mach number ($M = \sqrt{\gamma p/\rho}$) equal to $M = 0.1$ and $M = 0,25$. Additionally, in order to have a reference to measure the effect of compressibility on particle acceleration, we consider an incompressible case (with $\nabla\cdot\mathbf{u} = 0$ and $\rho =$ a uniform constant).

The magnetic and velocity fields are here expressed in Alfvén speed units; a characteristic plasma velocity is given by the parallel Alfvén wave velocity along the mean magnetic field $v_A = B_0/\sqrt{4\pi\rho_0}$. An Alfven speed based on field fluctuations can also be defined as $v_0 = \sqrt{< b^2 > /4\pi\rho_0}$. We take v_0 as a unit for velocity and magnetic field fluctuations. We use the turbulence correlation length L as unit length. The unit timescale t_0 is derived from the unit length and the fluctuation Alfven speed $t_0 = L/v_0$. For equipartition of velocity and magnetic field fluctuation energy, the eddy turnover time also equates to the time scale t_0.

The MHD equations are solved numerically using a Fourier pseudospectral method with periodic boundary conditions in a cube of size $L_{box} = 2\pi L$; this scheme ensures exact energy conservation for the continuous time spatially discrete equations[16]. The discrete time integration is done with a high-order Runge-Kutta method, and aresolution of (256^3) Fourier modes is considered. For the kinematic Reynolds number $R = v_0 L/\nu$ and the magnetic Reynolds number $R_m = v_0 L/\eta$, we take $R = R_m = 1000$, which are limited here by available spatial resolution. We consider a decaying simulation from an initial state with the kinetic and magnetic field fluctuations populating an annulus in Fourier k-space defined by a range of wavenumbers with $3 \le k \le 4$, constant amplitudes, and random phases.

When the turbulence is fully-developed a broad range of scales develops, from the outer scale L to the dissipation scale $l_d \approx L/32$. We then employ this turbulent (fixed) MHD state in which to evolve the test particles. The behavior of a test particle in an electromagnetic field is described by the nonrelativistic particle equation of motion:

$$\frac{d\mathbf{v}}{dt} = \alpha(\mathbf{E} + \mathbf{v}\times\mathbf{B}), \qquad \frac{d\mathbf{r}}{dt} = \mathbf{v}. \tag{5}$$

The nondimensional electric field $\mathbf{E}$ is obtained from Ohm's law normalized with $E_0 = v_0 B_0/c$ as follows:

$$\mathbf{E} = -\mathbf{u}\times\mathbf{B} + \frac{\mathbf{j}}{R_m}. \tag{6}$$

Finally the adimensional parameter α relates particles and MHD field parameters:

$$\alpha = Z\frac{m_p}{m}\frac{L}{\rho_{ii}}, \tag{7}$$

where ρ_{ii} is the proton inertial length given by $\rho_{ii} = m_p c/(e\sqrt{4\pi\rho_0})$. The inverse $1/\alpha$ represents the noninal gyroradius, in units of L and with velocity v_0 and measures the range of scales involved in the system (from the outer scale of turbulence to the particle gyroradius). One could expect a value $\alpha \gg 1$ specially for space physics and astrophysical plasmas. This represent a huge computational challenge due to numerical limitations. As

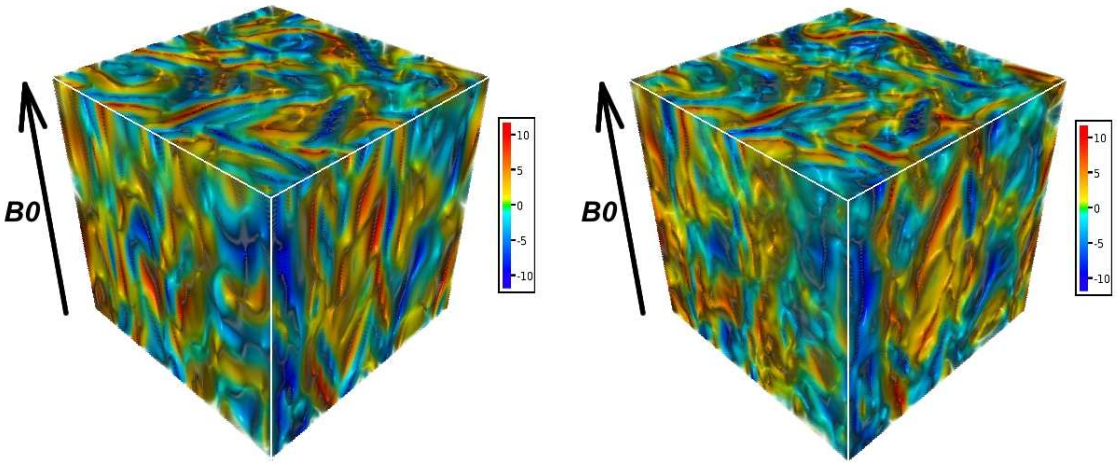

FIG. 1. Three-dimensional view of the parallel current density $J_z(x, y, z)$. (Left) Incompressible and (Right) Compressible case with Mach number $M = 0.25$ at $t/t_0 = 2$.

stated above, we consider here a dissipation length scale $l_d = L/32$, which is also of the order of the current sheet thickness.

In the fixed MHD turbulence state, 10000 test particles are randomly distributed in the computational box and the equation of motion of particles subject to the MHD electromagnetic field are solved using a second-order Runge-Kutta method. Furthermore, we use high order spline interpolation to compute the field values on each particle position.

Particles are initialized with Gaussian velocity distribution function with a root mean square (rms) value of the order of the Alfven velocity. It is well known that the particle gyroradius has a significant influence on acceleration, and our aim in this paper is to explore the compressibility effect on acceleration of large gyroradius and small gyroradius particles. In the next section we show two different compressible cases with Mach number $M = 0.25$ and $M = 0.1$, and an incompressible case. In all the cases the mean magnetic field is set to $B_0 = 10$. We present the behavior of protons with a nominal (speed v_0) gyroradius 1/32, and electrons ($m_e = m_p/1836$) with nominal gyroradius 1/58752.

III. RESULTS:

In Figure 1 a three-dimensional view of the z-component of the current density $J_z(x, y, z)$ is shown at $t = 2.5t_0$ for an incompressible case and a compressible case with $M = 0.25$. It is observed that current sheets are aligned in the direction of the guide magnetic field. It can be seen that in both cases the structures are similar, but more corrugated in the compressible case and smoother in the incompressible one. It is worth mentioning that we used the same initial conditions for all the simulations. Coherent structures like these show the natural tendency of the MHD equations to develop strong gradients leading to many reconection zones, which is well known to be one of the mechanisms behind charged particle acceleration.

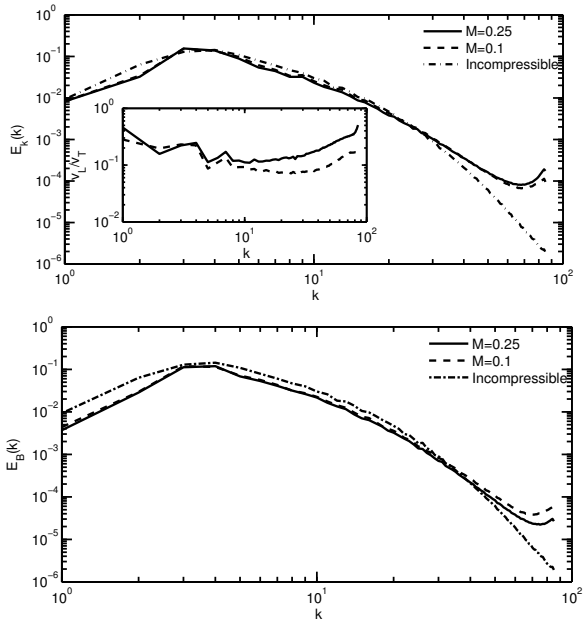

FIG. 2. (Top) Kinetic energy spectrum for compressible cases with Mach numbers $M = 0.25$ (solid line), $M = 0.1$ (dashed line), and incompressible case (dashed-dot line); the inset shows the ratio between solenoidal and irrotational (compressive) components of the velocity field for compressible runs. (Bottom) Magnetic energy spectrum for the three cases mentioned before, using the same labels.

Figure 2 shows the spectrum of kinetic (top) and magnetic energy (bottom) for the compressible cases with

$M = 0.25$ and $M = 0.1$ cases, and the incompressible case. In the inertial range there are almost no differences between the compressible and incompressible energy spectra for both magnetic and velocity fields, although slightly more energy at large scales is observed in the incompressible case. On the other hand, at wavenumbers beyond the dissipation scale (that is, for $k \geq 32$), an excess of energy is observed as the Mach number is increased. This feature is more evident for the kinetic energy spectrum than for the magnetic energy spectrum. Since protons mostly interact with structures of that size, this can be an important effect on proton acceleration.

In order to explore the importance of compressible effects on MHD fields, we make a Helmholtz decomposition of the velocity field, presented in the inset in Fig 2, where $v_T(\mathbf{k}) = (\mathbf{I} - \hat{\mathbf{k}}\hat{\mathbf{k}})\ \mathbf{u}(\mathbf{k})$ represents the solenoidal (incompressible) part and $v_L(\mathbf{k}) = u(\mathbf{k}) - v_T(\mathbf{k})$ is the irrotational (compressive) component. It is observed that at high k the velocity field spectrum is strongly compressive, and that compression becomes more prominent at higher turbulent Mach number.

Protons. Figure 3 shows the time evolution for the mean value of the perpendicular $v_\perp = \sqrt{v_x^2 + v_y^2}$ (top) and parallel $v_\parallel = v_z$ (bottom) proton velocity, relative to B_0, for the compressible ($M = 0.25$, $M = 0.1$) cases and the incompressible case. The typical acceleration process observed in previous studies is evident, proton are accelerated perpendicularly with respect to B_0, while they are less accelerated parallely.

Moreover, the compressibiliy effect on particle acceleration is clearly observed. Protons are highly accelerated as compressibility of the fluid increases for both perpendicular and parallel directions. Acceleration of protons is also observed in the incompressible case (see inset plot) but the value of the velocity reached at the end of the simulation is much lower than in both compressible cases, even with relatively small values of the Mach number M as the ones considered here.

Figure 4 shows the probability distribution function (PDF) of the perpendicular x-component (top) and of the parallel z-component (bottom) of the electric field for the compressible and incompressible cases. The PDF shows that, as compression increases, long tails in the distribution arise and higher values of the perpendicular electric field are achieved. Additionally, the core part of the distribution function for the incompressible case is thicker than for the compressible cases. On the other hand, the PDF of the parallel electric field shows very little effect of increasing compressibility.

In order to better understand the dynamics of protons, in Figure 5 we show the current density $J_z(x, y, z)$ together with the trajectory of one of the most energetic protons, for the compressible $M = 0.25$ case. The visualization was done using the software VAPOR[6]. It is observed that on the surrounding of the particle trajectory there are many current sheets, which contribute to the proton energization.

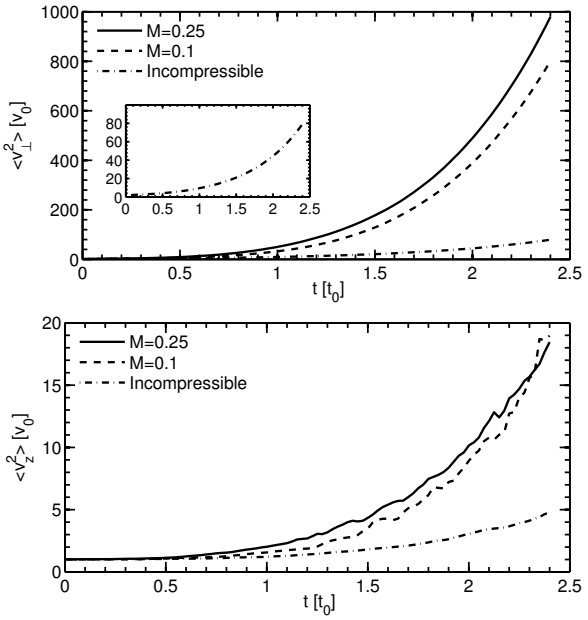

FIG. 3. Particle mean square velocity as a function of time: (Top) Proton perpendicular velocity $v_\perp = \sqrt{v_x^2 + v_y^2}$ for two different Mach number cases, $M = 0.25$ (solid line), $M = 0.1$ (dashed line), and the incompressible case (dash-dot line). (Bottom) Proton parallel velocity $v_\parallel = v_z$ for $M = 0.25$, $M = 0.1$, and incompressible case, with the same labels for the lines.

Figure 6 shows the values of quantities following the trajectory of the most energetic proton, that is, the most energetic proton is identified and the values of several quantities along the trajectory of this proton are obtained: (a) the current density J_z, (b) electric field components E_x, E_y, E_z, (c) proton velocity components v_x, v_y, v_z and (d) root mean square displacement of the proton. The panels on the left correspond to the compressible $M = 0.25$ case, and the panels on the right correspond to the incompressible case.

It is observed that when there is a change of the sign in the current density J_z, there is also an increment in the perpendicular components of the electric field that the particle experience, and concurrently there is an increment of the proton velocity. This situation is repeatedly observed in time as the energy of the proton increases.

A possible explanation for the change of sign in the current density is that the particle is entering and leaving two neighboring current sheets with different polarities while experiencing a strong perpendicular electric field between those current sheets. The perpendicular electric field is stronger as the compression of the fluid increases (this can be noticed by comparing panels on the left and right of Figure 6). Consequently the velocity increment is larger in the compressible case than in the incompressible case. This situation can be generalized for many particles in the simulation, resulting in the increase of the root mean square velocity for the ensemble of particles.

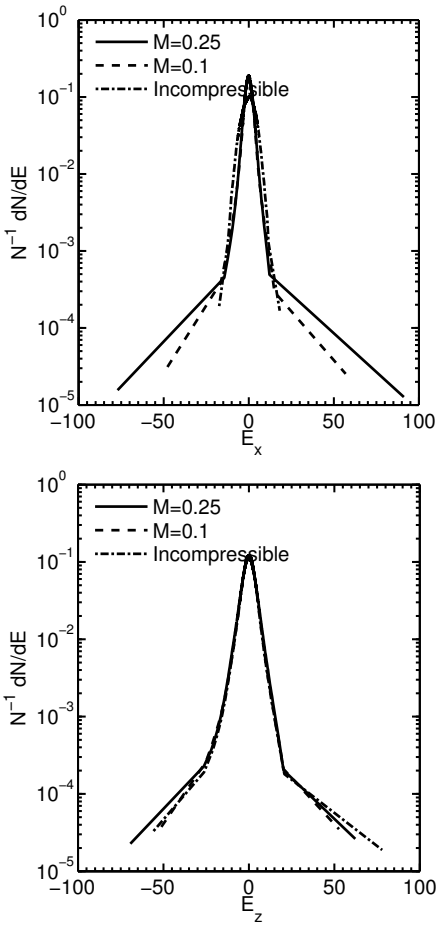

FIG. 4. Probability density function of electric field components in the simulation. (Top) Perpendicular x-component for $M = 0.25$ (solid line), $M = 0.1$ (dashed line), and incompressible (dash-dot line). (Bottom) Parallel z-component of the electric field using the same labels.

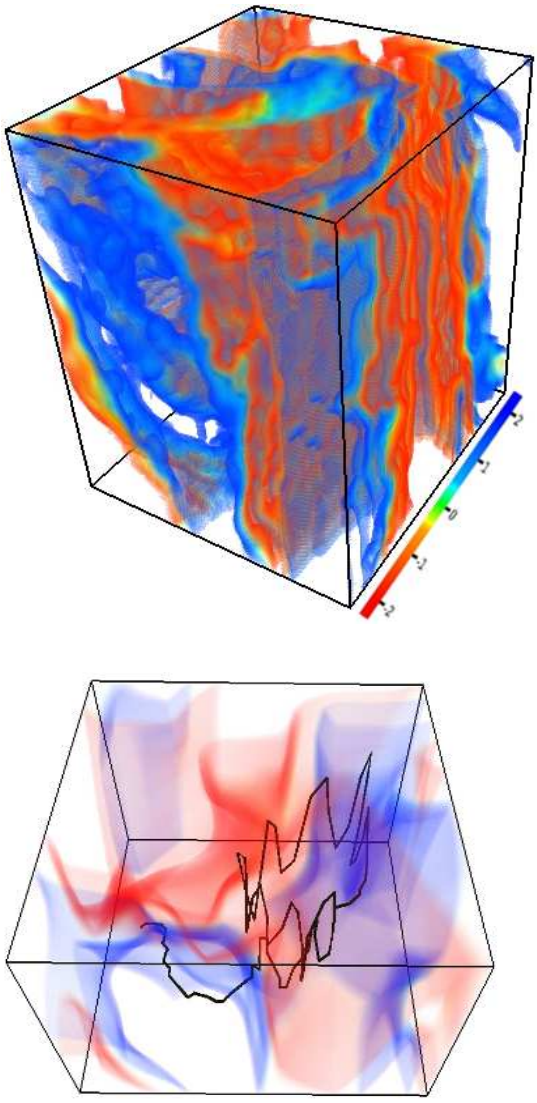

FIG. 5. (Top) View of the parallel current density $J_z(x, y, z)$. (Bottom) Trajectory of one of the most energetic protons; the z-component of the current density is shown in the transparent volume rendering.

The reason for greater perpendicular electric field for the compressible cases can be understood in terms of the magnetic flux pileup that accompanies the interaction of adjacent flux tubes in turbulence[18]. While current sheets typically form between interacting flux tubes, when the flux tubes are driven together by the turbulent flow, there is also frequently a magnetic flux pileup near the boundary. This compression of the magnetic field occurs in the incompressible case as well, but clearly can be greater when the material elements themselves are compressible. The pileup phenomenon is readily seen to be associated with reversal of the electric current density. Furthermore, the parallel magnetic flux increases due to this compression, requiring a circulation of the perpendicular electric field vector, thus setting the scene for betatron acceleration[7].

Electrons. Figure 7 shows the time evolution for the perpendicular (top) and z-component (bottom) of electron rms velocity for the compressible ($M = 0.25$, $M = 0.1$) and incompressible cases.

It should be mentioned that we are showing a short time simulation of electrons here. This is due to the high computational cost of integrating the trajectory of electrons in a flow, as electrons require a small time step (to represent a physical small gyroradius). The total time reached in the electron simulations is of the order of almost 3000 electron gyroperiods.

Electrons present the typical parallel energization reported in previous works. Besides, there is no evidence that compression of the MHD fields enhance the electron acceleration and electrons gain almost the same energy regardless the compressible level of the fluid.

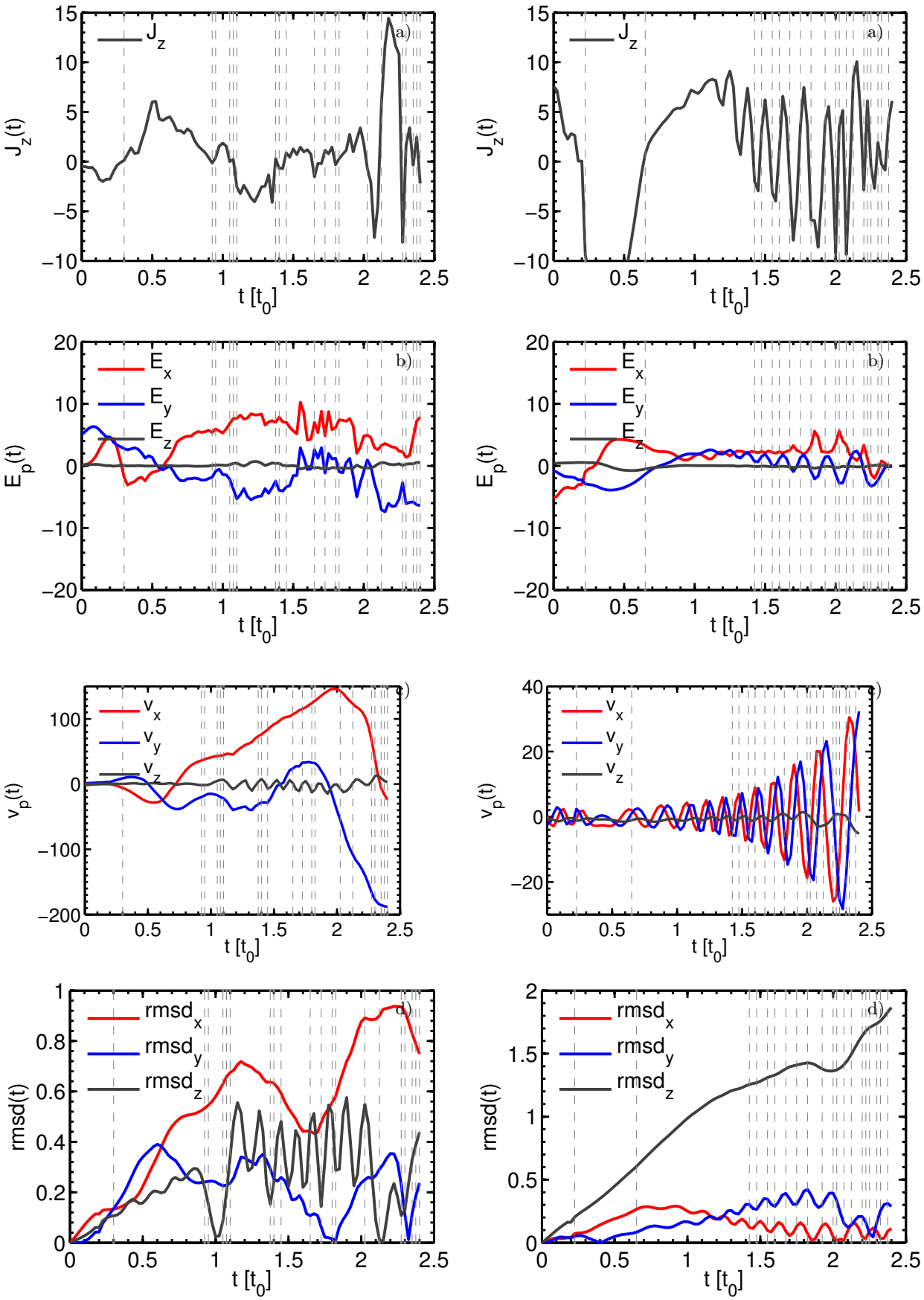

FIG. 6. (a) Parallel current density, (b) the three components of the electric field, (c) velocity components, and (d) rms displacement as function of time for the most energetic particle: (Left) compressible $M = 0.25$ case and (Right) incompressible case. The gray vertical dashed-lines show the moments when current is reversed.

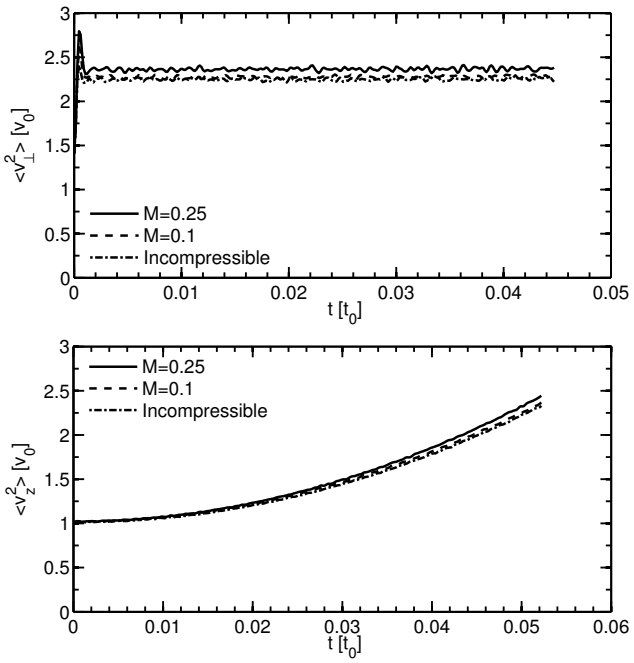

FIG. 7. (Top) Time evolution of the perpendicular rms velocity for electrons, for the compressible cases with $M = 0.25$ (solid line), $M = 0.1$ (dashed line), and the incompressible case (dot-dashed line). (Bottom) Time evolution of the parallel rms velocity for electrons, using the same notation.

Since the gyradius of electrons is smaller than any of the length scales of structures in the fields, when electrons find a current sheet they travel along magnetic field lines and there is not so much difference between compressible and incompressible cases.

Also, the perpendicular rms velocity shows that electrons are initially accelerated but quickly exhibit a constant perpendicular energy. Constant perpendicular energy is consistent with near conservation of the magnetic moment, which is one of the adiabatic invariants of charged particle dynamics in a magnetic field.

It is important to remark that over longer timescales, of the order of many turnover times, electrons can obtain very high parallel energy, and it is likely that the motion will no longer be adiabatic. In that case, electrons can reach other regions and interact with structures that generate other possible acceleration mechanisms, such as those that involve pitch angle-scattering, betatron acceleration, etc.

IV. DISCUSSION:

We have investigated the effect of compressible MHD turbulence on particle energization, using test particle simulations in frozen electromagnetic fields obtained from direct numerical solutions of the MHD equations. We found noticed that compression affects only the energization of large particle gyroradius (of the order of the dissipation length), and no effect of compression for small particle gyroradius is observed.

Protons are accelerated by the perpendicular electric field generated on the interface of current sheets, and they gain substantial energy as they encounter these structures. Moreover the perpendicular electric field between current sheets is greater as compression of the fluid increases, leading to a higher proton acceleration.

On the other hand, small gyroradii particles remain magnetized and gain parallel energy as they travel along magnetic field lines almost aligned with B_0. No compression effect is noted for these kind of particles and this is because the compressible modes in magnetohydrodynamics are perpendicular propagation modes ($k \perp B_0$), and as a result no difference in the parallel electric field obtained from static MHD fields is presented.

In this paper we analyzed the case of weakly compressible turbulence, often appropriate to study the solar wind and other astrophysical scenarios, even though these plasmas can sometimes attain a strongly compressible state ($M \geq 1$). we can thus conclude that at least for low turbulent Mach number, compression can enhance particle energization associated with coherent structures and therefore it has important implications for the study of particle acceleration by turbulent fields. In the incompressible case, which is the limit of infinite sound wave velocity, protons can still be accelerated, but less than in the compressible case. The incompressible case thus served as a reference to measure the influence of compression on particle acceleration. Also, the incompressible case can represent a real physical scenario, like the fast solar wind which might energize particles as well[19].

We close with a remark concerning the importance of trapping effects in acceleration of particles to higher energies in compressible turbulence. In general for effective energization the particles must be exposed to a suitable electric field, but also the trajectory of the particle must allow a long exposure time of the particle to the accelerating field.

In the present case, parallel acceleration of electrons occurs when their gyroradii are small compared to the width of mean field-aligned current channels, as noted previously by[8]. Analogous trapping effects due to confinement in magnetic "islands" has been noted in various systems from two dimensional MHD[1] to fully kinetic PIC simulations[9]. In those scenarios small gyroradius particle are trapped for a period of time sufficient for them to experience substantial parallel energization. Depending on parameters this may be either heating (more particles, lower energies) or acceleration (less particles but higher energy). On the other hand, protons, having larger gyroradius, will not be easily trapped in current channels, which often are a few proton inertial scales in width.

The perpendicular acceleration mechanism described previously[7,8] and elaborated on here, provides a way to accelerate protons (and heavier ions) due to pependicular electric fields. The region of interaction between

flux tubes provides the possibility of generating regions of effective acceleration that may lie between reversing currents. Although these may be very complex regions in three dimensions, in a simplified two dimensional picture, these can be flux pileup regions with gradients of the perpendicular electric field . This transversed compression of the magnetic field may occur even when the turbulence is incompressible. However, it is intuitively clear that compressibility will permit greater pileup and greater perpendicular electric field gradients. In addition, to produce an efficient accelerator, the particles must also be trapped in the accelerating region for sufficient time. The present numerical experiments also suggest that compressibility of the turbulence, acting near and within the regions between reversing currents, may provide substantially enhanced trapping for some particles. This is needed to explain the significantly greater perpendicular acceleration observed here when the turbulence is compressible.

ACKNOWLDEGMENTS

We acknowledge support from the following grants UBACyT 20020110200359, 20020100100315, and PICT 2011-1529, 2011-1626, 2011-0454.

W.H. Matthaeus is partially supported by NASA LWS-TRT grant NNX15AB88G,Grand Challenge Research grant NNX14AI63G, the Solar Probe Plus mission through the Southwest Research Institute ISOIS project D99031L.

[1] John Ambrosiano, William H. Matthaeus, Melvyn L. Goldstein, and Daniel Plante. Test particle acceleration in turbulent reconnecting magnetic fields. *Journal of Geophysical Research: Space Physics*, 93(A12):14383–14400, 1988. ISSN 2156-2202. doi: 10.1029/JA093iA12p14383. URL http://dx.doi.org/10.1029/JA093iA12p14383.

[2] Kaspar Arzner and Loukas Vlahos. Particle acceleration in multiple dissipation regions. *The Astrophysical Journal Letters*, 605 (1):L69, 2004. URL http://stacks.iop.org/1538-4357/605/i=1/a=L69.

[3] Benjamin D. G. Chandran. *The Astrophysical Journal*, 599(2): 1426, 2003. URL http://stacks.iop.org/0004-637X/599/i=2/a=1426.

[4] Benjamin D. G. Chandran and Jason L. Maron. *The Astrophysical Journal*, 603(1):23, 2004. URL http://stacks.iop.org/0004-637X/603/i=1/a=23.

[5] Jungyeon Cho and A. Lazarian. *The Astrophysical Journal*, 638 (2):811, 2006. URL http://stacks.iop.org/0004-637X/638/i=2/a=811.

[6] John Clyne, Pablo Mininni, Alan Norton, and Mark Rast. Interactive desktop analysis of high resolution simulations: application to turbulent plume dynamics and current sheet formation. *New Journal of Physics*, 9(8):301, 2007. URL http://stacks.iop.org/1367-2630/9/i=8/a=301.

[7] S. Dalena, A. F. Rappazzo, P. Dmitruk, A. Greco, and W. H. Matthaeus. *The Astrophysical Journal*, 783(2):143, 2014. URL http://stacks.iop.org/0004-637X/783/i=2/a=143.

[8] Pablo Dmitruk, W. H. Matthaeus, and N. Seenu. *The Astrophysical Journal*, 617(1):667, 2004. URL http://stacks.iop.org/0004-637X/617/i=1/a=667.

[9] J. F. Drake, M. Swisdak, H. Che, and M. A. Shay. Electron acceleration from contracting magnetic islands during reconnection. *Nature*, 443(7111):553–556, October 2006. ISSN 0028-0836. URL http://dx.doi.org/10.1038/nature05116.

[10] ENRICO Fermi. *Phys. Rev.*, 75:1169–1174, Apr 1949. doi: 10.1103/PhysRev.75.1169. URL http://link.aps.org/doi/10.1103/PhysRev.75.1169.

[11] Lange, S., Spanier, F., Battarbee, M., Vainio, R., and Laitinen, T. *A&A*, 553:A129, 2013. doi:10.1051/0004-6361/201220804. URL http://dx.doi.org/10.1051/0004-6361/201220804.

[12] A. Lazarian, L. Vlahos, G. Kowal, H. Yan, A. Beresnyak, and E.M. de GouveiaDalPino. *Space Science Reviews*, 173(1-4):557–622, 2012. ISSN 0038-6308. doi:10.1007/s11214-012-9936-7. URL http://dx.doi.org/10.1007/s11214-012-9936-7.

[13] Jacob W. Lynn, Eliot Quataert, Benjamin D. G. Chandran, and Ian J. Parrish. *The Astrophysical Journal*, 777(2):128, 2013. URL http://stacks.iop.org/0004-637X/777/i=2/a=128.

[14] W. H. Matthaeus, J. J. Ambrosiano, and M. L. Goldstein. *Phys. Rev. Lett.*, 53:1449–1452, Oct 1984. doi: 10.1103/PhysRevLett.53.1449. URL http://link.aps.org/doi/10.1103/PhysRevLett.53.1449.

[15] W. H. Matthaeus, Minping Wan, S. Servidio, A. Greco, K. T. Osman, S. Oughton, and P. Dmitruk. Intermittency, nonlinear dynamics and dissipation in the solar wind and astrophysical plasmas. *Philosophical Transactions of the Royal Society of London A: Mathematical, Physical and Engineering Sciences*, 373 (2041), 2015. ISSN 1364-503X. doi:10.1098/rsta.2014.0154.

[16] Pablo D. Mininni, Duane Rosenberg, Raghu Reddy, and Annick Pouquet. A hybrid mpiopenmp scheme for scalable parallel pseudospectral computations for fluid turbulence. *Parallel Computing*, 37(67):316 – 326, 2011. ISSN 0167-8191. doi:http://dx.doi.org/10.1016/j.parco.2011.05.004. URL http://www.sciencedirect.com/science/article/pii/S0167819111000512.

[17] Reinhard Schlickeiser and James A. Miller. *The Astrophysical Journal*, 492(1):352, 1998. URL http://stacks.iop.org/0004-637X/492/i=1/a=352.

[18] S. Servidio, W. H. Matthaeus, M. A. Shay, P. Dmitruk, P. A. Cassak, and M. Wan. Statistics of magnetic reconnection in two-dimensional magnetohydrodynamic turbulence. *Physics of Plasmas*, 17(3):032315, 2010. doi: http://dx.doi.org/10.1063/1.3368798. URL http://scitation.aip.org/content/aip/journal/pop/17/3/10.1063/1.3368798.

[19] Bogdan Teaca, Martin S. Weidl, Frank Jenko, and Reinhard Schlickeiser. *Phys. Rev. E*, 90:021101, Aug 2014. doi: 10.1103/PhysRevE.90.021101. URL http://link.aps.org/doi/10.1103/PhysRevE.90.021101.

[20] Martin S. Weidl, Frank Jenko, Bogdan Teaca, and Reinhard Schlickeiser. *The Astrophysical Journal*, 811(1):8, 2015. URL http://stacks.iop.org/0004-637X/811/i=1/a=8.